Ultrasonic attenuation via energy diffusion channel in disordered conductors

Alexander Shtyk[1,2,3] and Mikhail Feigel'man[1,2]
[1]*L. D. Landau Institute for Theoretical Physics, Chernogolovka, Moscow region, Russia*
[2]*Moscow Institute of Physics and Technology, Dolgoprudny, Moscow region, Russia*
[3]*Department of Physics, Harvard University, Cambridge, Massachusetts 02138, USA*
(Received 25 June 2015; published 2 November 2015)

We predict an existence of a dissipation channel leading to attenuation of ultrasound in disordered conductors and superconductors with perfect electroneutrality. It is due to slow diffusion of thermal energy. We show that in doped silicon ultrasound attenuation may be enhanced by a factor about 100. A similar effect is also studied for s-wave and d-wave superconductors. The latter case is applied to BSCCO family where a strong enhancement of the ultrasound attenuation is predicted. For usual s-wave superconductors, this dissipation channel might be important for very low-electron-density materials near the BCS-BEC crossover.

DOI: 10.1103/PhysRevB.92.195101 PACS number(s): 71.10.−w, 62.80.+f, 74.25.Ld

I. INTRODUCTION AND MODEL

Ultrasonic attenuation in metals has already been studied for a long time [1–5] and may seem to be fully understood. The ratio of ultrasound attenuation rate $\alpha(\omega)$ to the sound frequency ω in a clean metal is small due to the adiabatic parameter $mk_F^3/\rho_m \ll 1$, where m is the electron mass, k_F is the Fermi wave vector, and ρ_m is the density of the material. The simplest model for electron-phonon interaction is the scalar vertex Frohlich model with an extension due to Migdal [6,7]. This model is applicable for clean metals. However, it is well known that the Frohlich model is not adequate when the phonon wavelength $2\pi/q$ exceeds the elastic electron mean free path l. In this *dirty* limit, when $ql \ll 1$, the conventional theory of electron-phonon interaction in a disordered conductor leads to the Pippard ineffectiveness condition (PIC) that tells that the ultrasonic attenuation at small wave vectors is suppressed by a factor $ql \ll 1$ [5].

Ultrasound attenuation is intrinsically related to the electron-phonon cooling power [8], which determines a possible scale of thermal inequilibrium between electrons and phonons. In particular, it was shown in Ref. [9] that the strong nonlinearities of current-voltage $I(V)$ characteristics observed in Ref. [10] are due to the overheating of electrons; moreover, a detailed study of the shape of $I(V)$ curves for different temperatures allows us to determine the rate of electron-phonon inelastic processes. It was found then that in a number of cases [10–12], the electron-phonon cooling rate is considerably higher than one would expect from the classical predictions based upon PIC considerations. Therefore it is important to reconsider the issues of both electron-phonon cooling rate and ultrasound attenuation in order to look for some effects, which may have been overlooked previously.

The PIC phenomenon results from strong Coulomb interaction that prohibits any charge imbalance in the system (perfect screening condition). Still, some mechanisms were found recently that increase the inelastic electron-phonon rate even in the presence of perfect screening. The first of them is present in a multiband electronic spectrum [8,13], the second one is realized when impurities do not quite follow the motion of the lattice [14]. Still another possibility is related with deviations from the perfect screening condition that become prominent in a strongly disordered conductor, where $k_F l$ is not very large [8,15]. The situations discussed in Refs. [8,13] for a multiband electron system or incomplete screening have one important common feature: it is the presence of some slowly diffusing mode of the electron liquid. For instance, it might be spin polarization in the case of spin-split bands in the presence of a strong magnetic field [8] or electron density, which can fluctuate due to the relative weakness of Coulomb repulsion [8,15].

In the present paper, we show that even in the simplest case of one-band electron spectrum and a perfect screening, the conventional PIC theory might still be insufficient. The reason is that electron liquid possesses an *additional* intrinsic diffusion mode that is present even under the condition of strict electroneutrality and single band. It is an *energy diffusion mode* that may play a role similar to the spin-polarization mode studied in Ref. [8]. Coupling of phonons to this diffusion mode results in an additional attenuation of longitudinal sound waves.

The rest of the paper is organized as follows. The model of electron-phonon interaction in the presence of disorder is defined in Sec. II. Ultrasonic attenuation due to the energy diffusion mode in normal conductors is studied in Sec. III. These results are extended to the usual s-wave superconductors in Sec. IV. Section V is devoted to the study of ultrasound attenuation in d-wave superconductors. After a description of the general approach in Sec. V A, in Sec. V B, we present new results for the ultrasound attenuation due to *local processes*, with a self-consistent treatment of disorder, which particularly reveals the consequences of the quantum criticality present in a d-wave state [16]; Sec. V C is devoted to the description of the energy diffusion mode in the d-wave case; the results for the ultrasound attenuation due to an energy diffusion channel are presented in Sec. V D. Our conclusions are present in Sec. VI. A number of technical details are contained in Appendices A–C.

II. MODEL OF ELECTRON-PHONON INTERACTION IN PRESENCE OF DISORDER

We consider a dirty conductor with an electron action

$$S_{\mathrm{el},n} = \int dt(d\boldsymbol{r})\psi_i^*[i\partial_t - (\xi(\boldsymbol{p}) + U(\boldsymbol{r}))]\psi_i, \qquad (1)$$

with U being a disorder potential and $i = \uparrow, \downarrow$ corresponding to spin indices. The electron-phonon interaction is given by [3–5,8]

$$S_{\text{el-ph},n} = \int dt(d\boldsymbol{r})\psi_i^*[(p_F v_F/d)\partial_\alpha u_\alpha(\boldsymbol{r}) - \partial_\alpha(u_\alpha(\boldsymbol{r})U(\boldsymbol{r}))]\psi_i, \tag{2}$$

where the first term describes interaction due to the modulations of ionic density n_{ion}. Bare electron-ion interaction is in fact of the form $[n_{\text{ion}}V_0(\boldsymbol{q})]\,\text{div}\,\mathbf{u}$, $V_0(\boldsymbol{q}) = 4\pi e^2/q^2$ being the bare Coulomb interaction. Under the condition of full electroneutrality, this bare potential can be reduced to the form $[n_{\text{el}}\cdot\nu^{-1}] \equiv [d\ln n_{\text{el}}/d\ln\rho] = [p_F v_F/d]$. This simple expression is valid only for the case of a single branch of electron spectrum [8]. In addition, one should keep in mind that the dynamic nature of the screening becomes important at frequencies [8] $\omega \sim Dq^2$. The second term of Eq. (2) corresponds to distortions of the disorder potential, the latter being described by a correlator

$$\langle U(\boldsymbol{r})U(\boldsymbol{r}')\rangle = u\delta(\boldsymbol{r}-\boldsymbol{r}'). \tag{3}$$

It can be shown, using a comoving frame of reference (Refs. [3–5,8], Appendix A), that the action in the form of Eq. (2) is equivalent to [8]

$$S^{\text{CFR}}_{\text{el-ph},n} \simeq \int dt(d\boldsymbol{r})\psi_i^*\Gamma_n^{\alpha\beta}(\partial_\beta u_\alpha)\psi_i, \tag{4}$$

with the vertex

$$\Gamma_n^{\alpha\beta} = [p_\alpha v_\beta - (p_F v_F/d)\delta_{\alpha\beta}], \tag{5}$$

where p_F, v_F are the Fermi momentum and velocity, and d is the dimensionality of the electron system. Throughout the paper, the Keldysh version [17–19] of the diagram technique will be used. For an introduction to the Keldysh technique, see the review in Ref. [19].

III. ULTRASOUND ATTENUATION IN NORMAL CONDUCTORS

Local processes. The attenuation rate $\alpha(\omega)$ is related with the imaginary part of the phonon self-energy,

$$\alpha(\omega) = \frac{1}{\rho_m\omega}\,\text{Im}\,\Sigma^A(\omega,q)\Big|_{\omega=sq}. \tag{6}$$

The local contribution to the ultrasonic attenuation is due to processes that involve the creation and annihilation of electron and phonon states on a spatial scale comparable to the elastic mean free path. Such a process is depicted by the diagram in Fig. 1(a) and leads to a well known [1–5] result [it can be obtained via the calculation of the diagram Fig. 1(a) with the vertices defined in Eq. (5)]:

$$\alpha_{n,l} = 2c_l\frac{\nu p_F^2}{\rho_m}Dq^2 \propto \omega^2, \tag{7}$$

where ν is the electron density of states per one spin, D is the diffusion coefficient, and $c_l = 2(d-1)/d(d+2)$ is just a numerical coefficient.

Energy diffusion processes. For local processes, information about the direction of electron motion is retained between the acts of absorption and emission of phonons, thus the averaging of the product of two vertices over the directions of momentum in the diagram [Fig. 1(a)] leads to an important result:

$$\langle\Gamma_n(\boldsymbol{p})\Gamma_n(\boldsymbol{p})\rangle_{\boldsymbol{p}} \sim p_F^2 v_F^2. \tag{8}$$

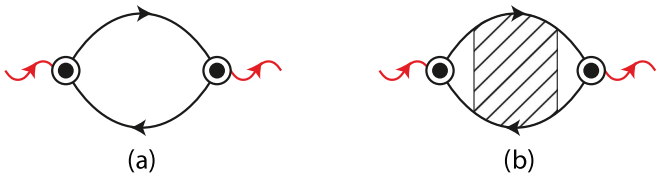

FIG. 1. (Color online) Phonon self-energy for (a) local processes and (b) diffusive channel, when phonon converts into diffusive mode. Throughout this paper, we use the Keldysh diagrammatic technique [17–19].

However, when diffusion processes are allowed, the same information is lost between absorption and emission of phonons. On a formal level, it is seen from the diagram [Figs. 1(b) and 2] where an impurity ladder is inserted into the diagram disconnecting the electron-phonon vertices. Multiple collisions with impurities hold electrons in the regions of phonon absorption and emission leading to an independent averaging of the interaction vertices Γ over the directions of momenta. That results in much smaller values of the effective vertex, which is now of the order of the temperature $T \ll p_F v_F$,

$$\langle\Gamma_n(\boldsymbol{p})\rangle_{\boldsymbol{p}} \sim \varepsilon \sim T. \tag{9}$$

This is the reason why diffusion modes are usually neglected in the electron-phonon interaction in disordered conductors.

It is convenient to define an effective electron-diffusion vertex that depends on the electron energy instead of a quickly relaxing momentum. Diagrammatically [see Figs. 1(b) and 2], there is always a block of two Green functions that stands in between the phonon and diffusive mode and results in averaging over the electron momentum. Therefore an effective phonon-diffusion vertex $\langle\Gamma\rangle_n$ may be defined with the help of the following integral representation:

$$\langle\Gamma\rangle_n^{\alpha\beta}(\varepsilon_-,\varepsilon_+) = \frac{1}{2\pi\nu\tau}\int(d\boldsymbol{p})G_-^R\big[\Gamma_n^{\alpha\beta}(\boldsymbol{p}_-,\boldsymbol{p}_+)\big]G_+^A, \tag{10}$$

where subscripts $\pm$ stand for $(\varepsilon \pm \omega/2, \boldsymbol{p} \pm \boldsymbol{q}/2)$, respectively. In general, the effective vertex depends on both energies $\varepsilon_\pm = \varepsilon \pm \omega/2$ but in the limit $\omega \ll \varepsilon \sim T$ the dependence on ω is

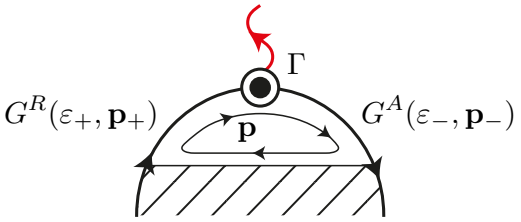

FIG. 2. (Color online) When coupled to a diffusive mode, the electron vertex is always averaged over the momentum $\boldsymbol{p}$ that goes in the block of two Green functions preceding the diffusion .

negligible. A new vertex $\langle\Gamma\rangle_n^{\alpha\beta}(\varepsilon)$ is then given by

$$\langle\Gamma\rangle_n^{\alpha\beta}(\varepsilon) = \varkappa\varepsilon\,\delta_{\alpha\beta}, \tag{11}$$

where

$$\varkappa = \frac{\partial(p v/d)}{\partial\varepsilon} \equiv \left(1 - \frac{p_F v_F}{d}\frac{\partial \ln \nu}{\partial\varepsilon}\right). \tag{12}$$

Diffusive electron modes evolve on a much larger timescales $\sim(Dq^2)^{-1}$ implying a more effective dissipation, despite a weak phonon-diffuson conversion. While the square of the vertex is smaller by the factor $(T/\varepsilon_F)^2$, the dissipation due to diffusion processes is enhanced by a factor $(ql)^{-2}$ (at the lowest frequencies the enhancement is saturated by a factor v_F^2/s^2, s being a sound velocity).

To the best of our knowledge, such processes for a single-band conductor under the condition of the perfect Coulomb screening had always been neglected so far. The corresponding diagram is shown in Fig. 1(b). Its evaluation leads to the following result [see also Eq. (6)], valid at $\hbar\omega \ll T$:

$$\alpha_{n,d}(\omega) = \int_0^\infty \left(d\varepsilon\frac{\partial f(\varepsilon,T)}{\partial\varepsilon}\right)\alpha_{n,d}^{(\varepsilon)}(\omega), \tag{13}$$

where $\alpha_{n,d}^{(\varepsilon)}(\omega)$ is the partial contribution of electrons with energies in the interval $(\varepsilon,\varepsilon+d\varepsilon)$,

$$\alpha_{n,d}^{(\varepsilon)}(\omega) = \frac{q^2}{\rho_m}(\varkappa\varepsilon)^2(2\nu\,\mathrm{Re}\,\mathcal{D}(\omega,q)). \tag{14}$$

Equation (14) contains a diffusion propagator $\mathcal{D}(\omega,q)$ (the corresponding diagrams are shown in Fig. 3) equal to

$$\mathcal{D}(\omega,q) = \frac{1}{-i\omega + Dq^2}, \tag{15}$$

where $\tau = l/v_F$ is an electron elastic scattering time and the diffusion coefficient $D = \tau v_F^2/d$. [Note that $\tau = (2\pi\nu u)^{-1}$ with electron density of states ν and u defined in Eq. (3).] The calculation of the integral in Eq. (13) leads to the following result for the ultrasound attenuation rate at frequency ω and temperature T:

$$\alpha_{n,d}(\omega) = \frac{2\pi^2}{3}\frac{\nu D}{\rho_m s^4}\frac{\varkappa^2 T^2\omega^2}{1+(D\omega/s^2)^2}. \tag{16}$$

It is useful to present it also in the form of the ratio of (16) to the "local" result, Eq. (7):

$$\frac{\alpha_{n,d}}{\alpha_{n,l}} = \frac{\pi^2}{3c_l}\left(\frac{\varkappa T}{p_F s}\right)^2\frac{\omega_c^2}{\omega_c^2+\omega^2}; \quad \omega_c = \frac{s^2}{D}. \tag{17}$$

The two mechanisms of dissipation lead also to different dependencies of the attenuation on the temperature and frequency: the "local" attenuation rate is only weakly T-dependent but grows as ω^2; on the other hand, the attenuation due to the "diffusive" mechanism is proportional to T^2. The dissipation due to the diffusive mechanism is frequency independent at high $\omega \gg \omega_c = s^2/D$ and goes as ω^2 at low frequencies. Equations (16) and (17) can be used in order to extract the value of the electron diffusion constant D from the data on the ultrasound attenuation.

For thermal phonons with $\hbar\omega \sim T$, the attenuation due to the diffusive channel is always small, $\alpha_{n,d} \ll \alpha_{n,l}$. However, for the ultrasonic attenuation at low frequencies, $\omega \ll T/\hbar$, the situation can be quite different, especially in doped semiconductors at moderate temperatures. Consider, for example, heavily doped Si with $n = 10^{20}$ cm^{-3}, $m = 0.36m_0$, $p_F l = 10$, and $s \approx 8\times10^5$ cm/s. At the temperature $T = 0.1E_F \approx 200$ K, one finds

$$\frac{\alpha_{n,d}}{\alpha_{n,l}} \approx 100, \quad f = 2\pi\omega \leqslant 10\ \mathrm{GHz}, \tag{18}$$

i.e., attenuation is enhanced by two orders of magnitude due to the contribution of the diffusive channel. Qualitatively, the same effect is expected to be at work at much larger temperatures, $T \gtrsim E_F$, as well, thus being especially relevant for semiconductors. However, such a regime requires a careful analysis that takes into account all the subtleties of the semiconductor physics, which goes well beyond the scope of the present paper.

IV. s-WAVE SUPERCONDUCTORS

A. Formulation of the model

We consider a BCS superconductor (SC) with an s-wave pairing and the microscopic interaction constant g,

$$S_{\mathrm{el,sc\text{-}int}} = \int dt(d\boldsymbol{r})[g\psi^*(\boldsymbol{r})\psi^*(\boldsymbol{r})\psi(\boldsymbol{r})\psi(\boldsymbol{r})]. \tag{19}$$

In the case of a dirty superconductor, it is convenient to define the Green function as

$$\begin{aligned}\check{G}^R_{\alpha\beta}(\varepsilon,\boldsymbol{p}) &= -i\langle\Psi_\alpha\overline{\Psi}_\beta\rangle \\ &= [(\varepsilon+i0)\check{\tau}_3 - \xi\check{\tau}_0 - \Delta(i\check{\tau}_2)]^{-1}_{\alpha\beta},\end{aligned} \tag{20}$$

where the 4-component spinor Ψ is defined as follows:

$$\Psi(\boldsymbol{p}) = \frac{1}{\sqrt{2}}\begin{pmatrix}\psi_{\boldsymbol{p}\uparrow}\\ \psi^*_{-\boldsymbol{p}\downarrow}\\ \psi_{\boldsymbol{p}\downarrow}\\ -\psi^*_{-\boldsymbol{p}\uparrow}\end{pmatrix}, \quad \overline{\Psi} = \Psi^+\check{\tau}_3. \tag{21}$$

The four-dimensional Nambu-Gor'kov space corresponds to the product of spin and particle-hole spaces. However, for our purposes, only the particle-hole subspace is relevant, as is evident from Eq. (20), where only particle-hole Pauli matrices $\check{\tau}$ are present. We will thus ignore the spin structure, effectively working with 2-component $\Psi,\overline{\Psi}$ spinors.

For a disordered s-wave superconductor, the self-consistent Born approximation gives [20]

$$\check{G}^R(\varepsilon,\boldsymbol{p}) = [\eta(\varepsilon)(\varepsilon\check{\tau}_3 - \Delta(i\check{\tau}_2)) - \xi\check{\tau}_0]^{-1} \tag{22}$$

with

$$\eta(\varepsilon) = \left(1 + \frac{i}{2\tau E}\right), \quad E = \sqrt{\varepsilon^2-\Delta^2}. \tag{23}$$

B. Energy density mode

1. Diffuson

Diffusion modes are described by the impurity ladder shown in Fig. 3. This ladder can be analyzed with the help of a Bethe-Salpeter equation,

$$(\widehat{\underline{\mathcal{D}}})^{-1}(\varepsilon,\omega,\boldsymbol{q}) = \widehat{\underline{1}} - \widehat{\underline{\Xi}}(\varepsilon,\omega,\boldsymbol{q}), \tag{24}$$

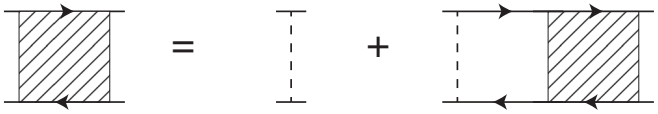

FIG. 3. Diffusive modes correspond to impurity ladders. The quantity $\mathcal{D}(\dots)$ in the text is given by the sum of this ladder, excluding one overall $(2\pi\nu\tau)^{-1}$ factor coming from the first impurity line.

with the self-energy

$$\underline{\widehat{\Xi}}(\varepsilon,\omega,\boldsymbol{q}) = u\int (d\boldsymbol{p})\,\check{G}^R(\varepsilon_-,\boldsymbol{p})\otimes\check{G}^A(\varepsilon_+,\boldsymbol{p}). \tag{25}$$

The Green function is a 2×2 matrix in the particle-hole space [the two-dimensional spin space is irrelevant, see Eq. (21)]. Thus $\underline{\widehat{\mathcal{D}}}$ and $\underline{\widehat{\Xi}}$ are matrices in a four-dimensional space constructed as a product of two two-dimensional particle-hole subspaces. These 4×4 matrices $\underline{\widehat{D}}$ and $\underline{\widehat{\Xi}}$ could be interpreted as superoperators acting on 2×2 operators such as an effective electron-phonon vertex $\check{\Gamma}$ [for an s-wave state $\check{\Gamma}$ is defined further in this chapter, see Eq. (30)]. For example, if $\check{A}$, $\check{B}$, and $\check{X}$ are 2×2 matrices, then $\check{Y}=\check{A}\check{X}\check{B}$ is as well a matrix of this type. This means that $\check{A}\otimes\check{B}$ describes a mapping $\check{X}\to\check{Y}$ thus indeed being a superoperator.

At zero external frequency and momentum the self-energy reads as follows:

$$\underline{\widehat{\Xi}} = \frac{1}{2}\check{\tau}_0\otimes\check{\tau}_0 + \frac{(\varepsilon\check{\tau}_3-\Delta(i\check{\tau}_2))\otimes(\varepsilon\check{\tau}_3-\Delta(i\check{\tau}_2))}{2(\varepsilon^2-\Delta^2)}. \tag{26}$$

Analyzing this matrix structure, one finds two massless modes corresponding to operators

$$\check{\tau}_0 \quad\text{and}\quad \varepsilon\check{\tau}_3-\Delta(i\check{\tau}_2). \tag{27}$$

The $\check{\tau}_0$ mode is symmetric in particle-hole space and corresponds to the charge density, while the asymmetric mode $\varepsilon\check{\tau}_3+\Delta(i\check{\tau}_2)$ corresponds to the energy density. The corresponding term in the matrix propagator defined in Eq. (24) is given by

$$(\underline{\widehat{\mathcal{D}}})(\varepsilon,\omega,q)\to\frac{1}{\tau}\mathcal{D}_s^{(\varepsilon)}(\omega,q), \tag{28}$$

where

$$\mathcal{D}_s^{(\varepsilon)}(\omega,q) = \frac{1}{[-i(E_+-E_-)+Dq^2]} \tag{29}$$

and $E_\pm=\sqrt{(\varepsilon\pm\omega/2)^2-\Delta^2}$. Charge density fluctuations are prohibited by the strong Coulomb interaction, so we should not consider them here.

Strictly speaking, there are two more diffusion modes of the "Cooperon" type, which are related to the charge conversion between the condensate and thermal excitations. Contrary to Eq. (25), these modes are constructed with a combination of Green functions of the type of $G^R(\varepsilon_-,\boldsymbol{p}_-)G^A(-\varepsilon_+,-\boldsymbol{p}_+)$. The corresponding propagator is proportional to $(-i(E_++E_-)+Dq^2)^{-1}$. It is important that in the limit $Dq^2\ll\sqrt{T\Delta}$, the contribution from these modes is much smaller than that of the energy diffusion channel, so we neglect the Cooperon channel in the following.

2. *Effective vertex*

When defining an equivalent phonon-diffuson vertex, we now have to pay attention to the matrix structure in the Nambu-Gor'kov space,

$$\langle\check{\Gamma}\rangle_s(\varepsilon) = u\int(d\boldsymbol{p})\check{G}^R_-\Gamma_n(\boldsymbol{p})\check{G}^A_+, \tag{30}$$

which modifies the vertex (11) into

$$\langle\check{\Gamma}\rangle_s(\varepsilon) = \varkappa(\varepsilon\check{\tau}_3-\Delta(i\check{\tau}_2))\delta_{\alpha\beta}. \tag{31}$$

We see that there is indeed no coupling between ultrasound and charge density modes. In the expression above, $u=(2\pi\nu\tau)^{-1}$.

We have used here the vertex of the same matrix structure as in the normal state, i.e. $\Gamma_n\check{\tau}_0$. The reason is that in the s-wave state there are no additional contributions to the vertex (except the one discussed right below, $\check{\Lambda}$ vertex). In the leading approximation, the electron-phonon vertex is given by the stress tensor of the electron system $p_\alpha\partial_\beta\check{H}$ (see Appendix A), plus an electromagnetic contribution representing screening that ensures electroneutrality. In the s-wave state, neither of these contributions is modified with respect to the normal state, since the part of the Hamiltonian related to the BCS gap functions is momentum independent $(\nabla_{\boldsymbol{p}}\check{\Delta})_\alpha=0$. Then, screening is proportional to quantity $[d\ln n_{\rm el}/d\ln\rho]$ that is not modified by the order parameter (in other words, the development of superconducting order parameter does not change the total number of particles).

Generally, an acoustic wave modifies the effective BCS coupling constant λ leading to an additional electron-phonon vertex. This vertex has the same matrix structure as the order parameter:

$$\check{\Lambda} = \varkappa_\Delta(\Delta\check{\tau}_1)\delta_{\alpha\beta} \tag{32}$$

with constant $\varkappa_\Delta$ being equal to

$$\varkappa_\Delta = -\frac{d\ln\Delta}{d\ln\rho}\underset{BCS}{=}-\frac{1}{\lambda}\left(\frac{d\ln\lambda}{d\ln\rho}\right). \tag{33}$$

Here, $\lambda=\nu g$ is a dimensionless BCS coupling constant. Below in this section, we consider the temperatures and all other relevant energy scales to be well below the gap $T,\omega,Dq^2\ll\Delta$.

Variations of λ arise either directly through the density of states ν or through interaction constant g,

$$\frac{d\ln\lambda}{d\ln\rho}=\frac{d\ln\nu}{d\ln\rho}+\frac{d\ln g}{d\ln\rho}. \tag{34}$$

Within our model $d\ln\nu/d\ln\rho=(p_Fv_F/d)(d\ln\nu/dE)$; it arises due to the shift of the chemical potential in the presence of an acoustic wave.

Defining the effective vertex $\langle\check{\Lambda}\rangle_s$ analogously to Eq. (30), we get

$$\langle\check{\Lambda}\rangle_s(\varepsilon) = \varkappa_\Delta\frac{\Delta^2}{2(\varepsilon^2-\Delta^2)}(\varepsilon\check{\tau}_3-\Delta(i\check{\tau}_2))\delta_{\alpha\beta}. \tag{35}$$

The effective vertex $\langle\check{\Lambda}\rangle_s$ is substantially enhanced due to the singular density of states, in contrast with the vertex $\langle\check{\Gamma}\rangle_s$.

C. Ultrasound attenuation due to energy diffusion

Similarly to the normal metal case, the contribution of the diffusion channel to the ultrasonic attenuation is given by the

following integral (assuming $\omega \ll T$):

$$\alpha_{s,d}(\omega) = \int_0^\infty \left(d\varepsilon \frac{\partial f(\varepsilon)}{\partial \varepsilon} \right) \alpha_{s,d}^{(\varepsilon)}(\omega), \tag{36}$$

where $\alpha_{s,d}^{(\varepsilon)}(\omega)$ is the partial contribution of quasiparticles with energies in the range $(\varepsilon, \varepsilon + d\varepsilon)$,

$$\alpha_{s,d}^{(\varepsilon)}(\omega) = \frac{q2}{\rho_m} \left(\varkappa E + \varkappa_\Delta \frac{\Delta^2}{2E} \right)^2 \left(2\nu_n \operatorname{Re} \mathcal{D}_s^{(\varepsilon)}(\omega, q) \right), \tag{37}$$

$\mathcal{D}_s^{(\varepsilon)}(\omega, q)$ being a diffuson in a superconducting state given by Eq. (29) and $E = \sqrt{\varepsilon^2 - \Delta^2}$. We have also added subscript n to the normal metal DOS ν_n to avoid a possible confusion. Note that the contribution due to variations of the effective BCS interaction constant (described by the vertex $\langle \check{\Lambda} \rangle$) is enhanced due to the singularity in the density of states at the gap edge, $\nu(\varepsilon)/\nu_n \simeq \Delta/\sqrt{\varepsilon^2 - \Delta^2}$.

Substitution of Eq. (37) into Eq. (36) and integration yields the final result for ultrasonic attenuation due to the energy diffusion channel in s-wave superconductors:

$$\alpha_{s,d}(\omega) = 2 \frac{\nu}{\rho_m D} \exp\left[-\frac{\Delta}{T} \right] \begin{cases} (\Delta/T)\left((\varkappa_\Delta/2)^2 \Delta^2 \ln \frac{T}{A(\omega)} + 2\varkappa\varkappa_\Delta \Delta T + 4\varkappa^2 T^2 \right) & \omega \gg \omega_c \sqrt{\frac{\Delta}{T}} \\ 2\left((\varkappa_\Delta/2)^2 \Delta^2 + 2\varkappa\varkappa_\Delta \Delta T + 8\varkappa^2 T^2 \right) \times \left(\frac{D\omega}{s^2} \right)^2 & \omega \ll \omega_c \sqrt{\frac{\Delta}{T}} \end{cases}, \tag{38}$$

where $A(\omega) \equiv \omega + \Delta(\omega_c/\omega)^2$ and $\omega_c = s^2/D$ is the crossover frequency in the normal state. Equations (38) were derived under the conditions

$$\omega, Dq^2 \ll T \ll \Delta \ll \tau^{-1} \ll p_F v_F \tag{39}$$

and contain two characteristic crossover frequencies, $\omega_{c,s1} = \omega_c(\Delta/T)^{1/2}$ and $\omega_{c,s2} = \omega_c^{2/3}\Delta^{1/3}$.

Note that $\omega_{c,s2}$ describes a weak logarithmic crossover that results from the DOS singularity in the superconducting state; (Δ/T) factor in the first line of Eq. (38) is the result of DOS behavior as well. This crossover exists only if $\omega_{c,s2} > \omega_{c,s1}$, or equivalently only for temperatures $T > (\Delta\omega_c^2)^{1/3}$. The frequency of the second crossover $\omega_{s,c2}$ can be small or large in comparison with $\omega_{s,c1}$, depending on the specific material.

To compare the attenuation due to the energy diffusion channel (38) with the one produced by the usual local processes in a superconducting state (we denote it as $\alpha_{s,l}$), note that the latter is proportional to the density of the normal electron-hole excitations [21]. Thus the ratio

$$\frac{\alpha_{s,l}}{\alpha_{n,l}} = \int_\Delta^\infty d\varepsilon \, \frac{\partial f(\varepsilon)}{\partial \varepsilon} \simeq 2 \exp\left(-\frac{\Delta}{T} \right), \tag{40}$$

so that $\alpha_{s,l} \propto \omega^2$ as in the normal state. At high frequencies $\omega \gg \omega_{c,s2}$, we thus find that the role of the energy diffusion channel grows with ω decrease:

$$\frac{\alpha_{s,d}}{\alpha_{s,l}} = \frac{1}{2c_l} \frac{1}{p_F^2 s^2} \left(\varkappa_\Delta^2 \frac{\Delta^3}{4T} \ln \frac{T}{A(\omega)} + 2\varkappa\varkappa_\Delta \Delta^2 + 4\varkappa^2 \Delta T \right) \times \left(\frac{\omega_c}{\omega} \right)^2. \tag{41}$$

In this frequency range, the attenuation due to energy diffusion has only a weak logarithmic frequency dependence; it also depends on the temperature in a nontrivial way that does not reduce to the T dependence of the normal electron density.

At the lowest frequencies, when $\omega \leqslant \omega_{c,s1}$, the frequency dependence of α_s is of the standard form, but the temperature dependence differs from that of the local contribution:

$$\frac{\alpha_{s,d}}{\alpha_{s,l}} = \frac{1}{c_l} \frac{1}{p_F^2 s^2} \left((\varkappa_\Delta/2)^2 \Delta^2 + \varkappa\varkappa_\Delta \Delta T + 8\varkappa^2 T^2 \right). \tag{42}$$

Inspection of the ratio (42) shows that usually it is rather small; an interesting exception is presented by superconductors with extremely low electron density, which are not far from the crossover to the regime of "local pairs." A particular example of this kind is presented by the recently discovered heavy-metal compound YPtBi [22] with a conduction electron density at temperatures about a Kelvin range as low as $n = 2 \times 10^{18}$ cm^{-3}. With the values of other parameters taken from Ref. [22] as $m = 0.15 m_0$, electron mean free path $l = 130$ nm, $T_c = 0.77$ K, $\omega_D = 200$ K, and sound velocity [23] $s = 2 \times 10^5$ cm/s, we find for $T = 0.2$ K the ratio of the energy diffusion contribution to the standard PIC result $\alpha_{s,l}$:

$$\frac{\alpha_{s,d}}{\alpha_{n,l}} \approx 1, \quad f = 2\pi\omega \leqslant 1 \text{ GHz}. \tag{43}$$

V. d-WAVE SUPERCONDUCTORS

A. Hamiltonian

We consider here strongly a model of an anisotropic d-wave superconductor and neglect the electron dispersion in the direction transverse to the layers. Then the order parameter depends on the direction of the momentum (Fig. 4) in the following way:

$$\Delta(\boldsymbol{p}) = \Delta_0(\cos p_x a - \cos p_y a), \tag{44}$$

where a is the lattice constant. At low temperatures $T \ll \Delta_0$, this leads to an angular dependence of the ultrasonic attenuation due to local processes. At the same time, the contribution of the diffusion channel is isotropic (see Fig. 5).

For a d-wave superconductor, the Green function is the same as for the s-wave case, up to a momentum dependence of the order parameter $\Delta \equiv \Delta(\boldsymbol{p})$:

$$\check{G}^R_{\alpha\beta}(\varepsilon, \boldsymbol{p}) = -i\langle \Psi_\alpha \overline{\Psi}_\beta \rangle = [(\varepsilon + i0)\check{\tau}_3 - \xi - (i\check{\tau}_2)\Delta]^{-1}, \tag{45}$$

The energy of excitations above the d-wave SC state vanishes at four nodal directions in the momentum space of the order parameter, see Fig. 5. Near these directions, the excitation spectrum can be linearized:

$$\xi = v_F k_1, \quad \Delta = v_g k_2, \tag{46}$$

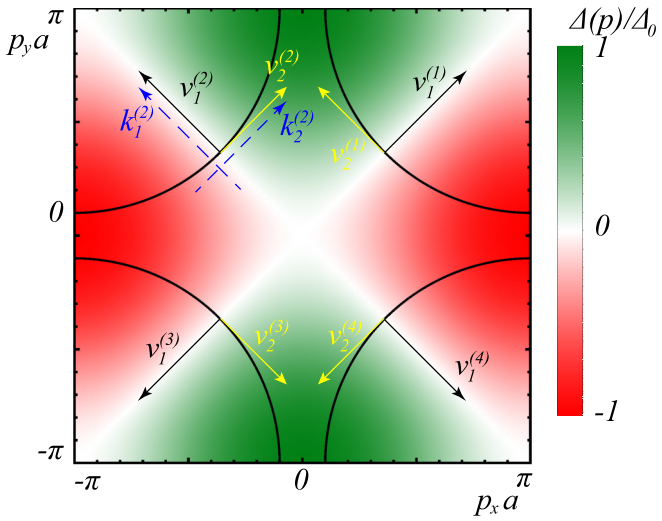

FIG. 4. (Color online) Schematic Fermi surface of a d-wave superconductor. The background color represents an order parameter $\Delta(\boldsymbol{p})$ with an angular dependence revealing four nodes on the Fermi surface. Each of them has its own electron Fermi $\boldsymbol{v}_1 = d\xi/d\boldsymbol{p}$ and gap $\boldsymbol{v}_2 = d\Delta/d\boldsymbol{p}$ velocities. We thus choose four different coordinate systems $(k_1,k_2)^{(i)}$(for clarity only one is shown) around each node with axes aligned with local electron Fermi and gap velocities. x and y directions correspond to [100] and [010] crystalline axes, respectively; a is the lattice constant.

where the momentum $\boldsymbol{k}$ is measured from the node, $\boldsymbol{k} = \boldsymbol{p} - \boldsymbol{p}_{\text{node}}$, and the basis is individual for each node (see the Fig. 4). Due to the presence of low-lying excitations, all thermal effects at $T \ll T_c$ are described by some power laws of T, instead of the exponential behavior in the s-wave case.

Now we should take into account a random disorder potential, which we consider in the white-noise limit:

$$\langle U(\boldsymbol{r})U(\boldsymbol{r}')\rangle = u\delta(\boldsymbol{r}-\boldsymbol{r}'). \tag{47}$$

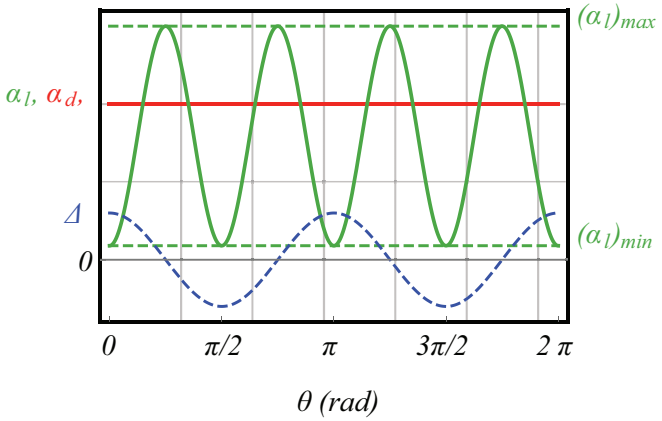

FIG. 5. (Color online) Schematic angular dependence of ultrasonic attenuation for local (α_l) and diffusive (α_d) processes. α_l exhibits a strong anisotropy with extremal values $(\alpha_l)_{\min}$ and $(\alpha_l)_{\max}$ shown by horizontal dashed lines. In contrast to local processes, the attenuation in the diffusion channel is isotropic. As a reference direction $\theta = 0$ we choose [110]. Minima of ultrasonic attenuation are observed in ±[100] and ±[010] directions, while maxima in ±[110] and ±[1 − 10]. The angular dependence of the gap $\Delta(\boldsymbol{k})$ is shown as well (dashed blue line).

Scattering by disorder results in renormalization of Green functions, leading both to a scattering rate γ and to renormalization of the energy: $\varepsilon \to \tilde{\varepsilon}$. In the self-consistent Born approximation, we find

$$\left\langle \check{G}^R_{\alpha\beta}(\varepsilon,\boldsymbol{p})\right\rangle = [(\tilde{\varepsilon}+i\gamma)\check{\tau}_3 - \xi\check{\tau}_0 + (i\check{\tau}_2)\Delta]^{-1}, \tag{48}$$

where $\tilde{\varepsilon}$ is related to a residue of the Green function,

$$\varepsilon \equiv Z(\varepsilon)\tilde{\varepsilon}(\varepsilon). \tag{49}$$

The quantities γ and $\tilde{\varepsilon}$ are to be determined by self-consistency equations [24]:

$$1 = K\left(\frac{\tilde{\varepsilon}}{\gamma}\arctan\frac{\tilde{\varepsilon}}{\gamma} + \ln\frac{\Delta_0}{\sqrt{\tilde{\varepsilon}^2+\gamma^2}}\right), \tag{50}$$

$$\varepsilon = K\frac{\tilde{\varepsilon}^2+\gamma^2}{\gamma}\arctan\frac{\tilde{\varepsilon}}{\gamma}, \tag{51}$$

where K is a dimensionless disorder strength,

$$K = \frac{Nu}{2\pi v_F v_g} \equiv N\frac{v_F}{v_g}G_n^{-1}. \tag{52}$$

Here, N is the number of valleys ($N = 4$), and G_n is the dimensionless conductance per layer in the normal state (in units of $e^2/\hbar$). The self-consistent Born approximation is valid as long as $K \ll 1$; since the ratio v_F/v_g is a large parameter (according to Ref. [25], it is about 20 for BSCCO superconductors), thus the normal-state conductance should be sufficiently large, $G_n \geqslant 100$, for this approach to be valid.

The asymptotic behavior of $\gamma(\varepsilon)$ and $Z(\varepsilon)$ is of particular interest, it is given by

$$\varepsilon \ll \gamma_0 : \ \gamma(0) = \Delta_0 e^{-1/K}, \quad Z(0) = K, \tag{53}$$

$$\varepsilon \gg \gamma_0 : \ \gamma = \frac{\pi}{2K}\frac{\varepsilon}{(\ln(\varepsilon/\gamma_0))^2}, \quad Z(\varepsilon) = K\ln(\varepsilon/\gamma_0), \tag{54}$$

where $\gamma_0 \equiv \gamma(0)$ is the scattering rate at the Fermi surface. The logarithmic energy dependencies of $\gamma(\varepsilon)$ and $Z(\varepsilon)$ are direct consequences of the quantum critical behavior of the quasiparticles in a d-wave state. Similar behavior takes place in graphene [26] where the conductivity acquires logarithmic corrections. Energies $\varepsilon \lesssim Z(0)\gamma(0) \sim K\Delta_0 e^{-1/K}$ (when $\tilde{\varepsilon} \lesssim \gamma_0$) require careful consideration that might imply a full-fledged renormalization group approach. We thus restrain ourselves to the intermediate temperature range $\gamma_0 \ll T \ll \Delta_0$.

To describe electron-phonon interaction, it is still sufficient to start from the electron stress tensor (5), but now the momentum dependence of the order parameter $\Delta(\boldsymbol{p})$ should be taken into account:

$$\check{\Gamma}_d^{\alpha\beta} = p_\alpha\partial_\beta\check{H} - \frac{p_F v_F}{2}\delta_{\alpha\beta} = \begin{pmatrix} (v_F p_F/2)+\varkappa\xi & (p_F+k_F)v_g(i\check{\tau}_2) \\ k_g v_F & -(p_F v_F/2)+\varkappa_\Delta\Delta(i\check{\tau}_2)\end{pmatrix}_{\alpha\beta}, \tag{55}$$

where we have used $\check{H} = \xi\check{\tau}_0 + \Delta(i\check{\tau}_2)$ and $\varkappa = d(p_F v_F/d)/d\xi$, and $\varkappa_\Delta = -d\ln\Delta/d\ln\rho$ are the same parameters as in the s-wave and normal cases.

B. Ultrasound attenuation due to local processes

Like previously, attenuation due to local processes in a d-wave superconductor can be depicted by the electron bubble diagram [Fig. 1(a)], the corresponding analytical expression reads as

$$\alpha_{d,l} = \frac{q^2}{2\rho_m \omega} \mathrm{Tr}\,[(f_+ - f_-)\check{\Gamma}(\check{G}^R_- - \check{G}^A_-)\check{\Gamma}(\check{G}^R_+ - \check{G}^A_+)], \tag{56}$$

where $\check{\Gamma}$ is an abbreviation for

$$\check{\Gamma} = e_\alpha \check{\Gamma}^{\alpha\beta}_{d,l} e_\beta \tag{57}$$

with e_α being a unit vector in the direction of phonon momentum q_α (while the polarization vector of longitudinal phonons is essentially the same as e_α). In contrast to normal and s-wave states, in a d-wave state, attenuation is essentially anisotropic due to the two strongly different velocities v_F and v_g and the symmetry of the order parameter.

A partial contribution of electrons with energies $(\varepsilon, \varepsilon + d\varepsilon)$ into the attenuation rate can be found in the form

$$\alpha^{(\varepsilon)}_{d,l}(\omega) = \frac{q^2}{2\pi^2 v_F v_g \rho_m}\left(1 + \frac{Z(\varepsilon)}{K}\right)\left(p_F^2 v_F^2 F(\theta)\right), \tag{58}$$

where the function $F(\theta)$ comes from electron-phonon vertices and describes the angular dependence of attenuation,

$$F(\theta) = \sin^2 2\theta + \left(\frac{v_g}{v_F}\right)^2 \cos^2 2\theta. \tag{59}$$

Integration of Eq. (58) over the electron energy [like in Eq. (13)] eventually leads to

$$\alpha_{d,l}(\omega) = \frac{F(\theta)}{2\pi^2}\frac{v_F}{v_g}\frac{p_F^2 \omega^2}{\rho_m s^2} \ln\frac{T}{\gamma_0}. \tag{60}$$

Comparing the result (60) with the attenuation in the (isotropic) normal state, we find

$$\frac{\alpha_{d,l}}{\alpha_{n,l}} = 2K F(\theta) \ln\frac{T}{\gamma_0}, \tag{61}$$

where K is the dimensionless measure of disorder defined in Eq. (52) and γ_0 is the scattering rate at the Fermi surface, see Eq. (53). Within the self-consistent Born approximation, the logarithmic behavior stops at temperatures $T \ll \gamma_0$, where one should just replace $\ln(T/\gamma_0) \to 2$ in Eq. (60).

The attenuation rate (60) possesses an unusual logarithmic temperature behavior $\propto \ln(T/\gamma_0)$ that does not correspond to naive expectations for the linear density of states, $\alpha \propto T$. The reason is that the electron scattering rate γ is intimately related to the electron density of states; the typical scattering rate decreases with T together with the typical DOS. Namely, Eq. (54) shows that at moderately high temperatures, $\gamma \propto T$ up to a logarithmic factor. Finally, the remaining logarithm $\ln(T/\gamma_0)$ in Eq. (54) is the result of quantum critical behavior. The situation with ultrasonic attenuation due to local processes in a d-wave state is completely analogous to the situation with logarithmic corrections to the conductivity of graphene [26].

C. Energy diffusion mode

1. Diffusion propagator

This section proceeds in a way almost identical to the s-wave case. The diffusion modes are described by a Bethe-Salpeter equation, Fig. 3,

$$(\widehat{\underline{D}})^{-1}(\varepsilon,\omega,q) = 1 - \widehat{\underline{\Xi}}(\varepsilon_-,\varepsilon_+,\boldsymbol{q}), \tag{62}$$

with a self-energy

$$\widehat{\underline{\Xi}}(\varepsilon,\omega,\boldsymbol{q}) = u\sum_{\text{nodes}}\int (d\boldsymbol{p})\check{G}^R_- \otimes \check{G}^A_+. \tag{63}$$

The energy density diffusion mode corresponds to the $\check{\tau}_3$ eigenvector and eigenvalue of the self-energy:

$$\widehat{\underline{\Xi}}(\varepsilon,\omega,\boldsymbol{q}) \to u\sum_{\text{nodes}}\int (d\boldsymbol{p})\mathrm{Tr}\,(\check{\tau}_3\check{G}^R_-\check{\tau}_3\check{G}^A_+). \tag{64}$$

Summation of the impurity ladder for the energy density mode thus gives

$$(\widehat{\underline{D}})(\varepsilon,\omega,\boldsymbol{q}) \to 2\gamma(\varepsilon)\mathcal{D}^{(\varepsilon)}_d(\omega,q), \tag{65}$$

where $\mathcal{D}^{(\varepsilon)}_d$ is a diffuson propagator in a d-wave state,

$$\mathcal{D}^{(\varepsilon)}_d(\omega,q) = \frac{1}{-i\omega + D^{(\varepsilon)}_d q^2}. \tag{66}$$

The diffusion coefficient is

$$D^{(\varepsilon)}_d = \frac{K + Z(\varepsilon)}{2\gamma(\varepsilon)}\langle v^2\rangle, \tag{67}$$

where $\langle v^2\rangle = (v_F^2 + v_g^2)/2 \simeq v_F^2/2$. Cooperon modes in a d-wave state are irrelevant at temperatures $T \gg \gamma_0$.

2. Effective vertex

The effective phonon-diffuson vertex is defined in a way similar to the s-wave state:

$$\langle\check{\Gamma}\rangle^{\alpha\beta}_d(\varepsilon) = u\sum_{\text{nodes}}\int (dp)\check{G}^R_+\check{\Gamma}^{\alpha\beta}_d(\boldsymbol{p})\check{G}^A_-. \tag{68}$$

Calculation of this vertex requires some caution, see Appendix for details. Eventually we get, similar to the normal metal state,

$$\langle\check{\Gamma}\rangle^{\alpha\beta}_d(\varepsilon) = \varkappa_*\varepsilon\check{\tau}_3\delta_{\alpha\beta}, \tag{69}$$

where $\varkappa_*$ is just the sum

$$\varkappa_* = \varkappa + \varkappa_\Delta. \tag{70}$$

The effective vertex describing coupling to the energy density mode turns out to be isotropic $\propto \delta_{\alpha\beta}$ once the summation over four nodes is performed. This happens despite the anisotropy of velocities for each node separately.

D. Ultrasound attenuation due to energy diffusion

We obtain the contribution of the diffusion processes in a complete analogy to the s-wave state:

$$\alpha_{d,d}(\omega) = \int_0^\infty \left(d\varepsilon\frac{\partial f(\varepsilon)}{\partial\varepsilon}\right)\alpha^{(\varepsilon)}_{d,d}(\omega), \tag{71}$$

where

$$\alpha^{(\varepsilon)}_{d,d}(\omega) = \frac{q^2}{\rho_m} \cdot \varkappa_*^2 \varepsilon^2 \cdot \left(2\nu_d(\varepsilon)\,\mathrm{Re}\,\mathcal{D}^{(\varepsilon)}_d(\omega,q)\right), \tag{72}$$

where $\nu_d(\varepsilon) = \gamma(\varepsilon)/\pi u$ is a density of states in a d-wave superconductor and $\varkappa_*$ is defined in Eq. (70). Then Eq. (72) gives

$$\alpha^{(\varepsilon)}_{d,d}(\omega) = \frac{1}{\pi^2}\frac{v_F}{v_g}\left(1 + \frac{Z(\varepsilon)}{K}\right)\frac{\varkappa_*^2\varepsilon^2}{\rho_m s^4}\frac{\omega^2}{1+\omega^2/\omega^2_{c,d}(\varepsilon)} \tag{73}$$

with a crossover frequency $\omega_{c,d}(\varepsilon) = s^2/D^{(\varepsilon)}_d$. We are interested only in the case of weak disorder $K \ll 1$ and temperatures $T \gg \gamma_0$. The effective crossover frequency which enters the result for the total attenuation, as given by Eq. (71), is

$$\omega_{c,d}(T) = \frac{\pi s^2}{2v_F^2}\frac{KT}{[1 - K\ln(\Delta_0/T)]^3}, \quad T \gg \gamma_0. \tag{74}$$

In Eq. (74), we have used the identity $K\ln(T/\gamma_0) \equiv 1 - K\ln(\Delta_0/T)$.

At low frequencies, the resulting attenuation rate has a $\propto T^2 \ln T$ temperature dependence:

$$\alpha_{d,d}(\omega) = \frac{1}{3}\varkappa_*^2\frac{v_F}{v_g}\frac{T^2\omega^2}{\rho_m s^4}\ln(T/\gamma_0), \quad \omega \ll \omega_{c,d}(T), \tag{75}$$

while for higher frequencies the attenuation behaves roughly as $\propto T^4$,

$$\alpha_{d,d}(\omega) = \frac{7\pi^4\varkappa_*^2}{60\rho_m v_F^3 v_g}\frac{KT^4}{[1 - K\ln(\Delta_0/T)]^5}, \quad \omega \gg \omega_{c,d}(T). \tag{76}$$

The additional two powers of temperature, $\propto T^4$ versus $\propto T^2$ in the normal state, are due to the nearly linear DOS at high energies, $\nu_d(\varepsilon) \propto \varepsilon$ up to logarithmic factors. Note that the energy dependence of the diffusion coefficient has the same origin, $D^{(\varepsilon)}_d \propto \gamma(\varepsilon) \propto \nu_d^{-1}(\varepsilon) \propto \varepsilon^{-1}$.

The contribution of the energy diffusion channel is especially prominent for directions that correspond to the minimum of the "local" attenuation rate [Fig. 5, Eq. (60)]. For such a direction at the lowest frequencies, when $\omega \leqslant \omega_{c,d}$, the ratio of the contributions from the energy diffusion and from a local channel is similar to that in the normal case,

$$\frac{\alpha_{d,d}}{(\alpha_{d,l})_{\min}} = \frac{2\pi^2}{3}\left(\frac{v_F}{v_g}\right)^2\frac{\varkappa_*^2 T^2}{p_F^2 s^2}. \tag{77}$$

For higher frequencies $\omega \gg \omega_{c,d}$ for the ratio of attenuation rates, we find

$$\frac{\alpha_{d,d}}{(\alpha_{d,l})_{\min}} = \frac{14\pi^4}{15}\left(\frac{v_F}{v_g}\right)^2\frac{\varkappa_*^2 T^2}{p_F^2 s^2}\left(\frac{\omega_c}{\omega}\right)^2, \tag{78}$$

All these results are valid as long as we are in the dirty limit $ql \ll 1$. This condition is equivalent to $D_d(T)q^2 \ll \gamma(T)$, which in turn gives $\omega \ll \omega_0^{(d)}(T)$,

$$\omega_0^{(d)}(T) \simeq \frac{s}{v_F}\frac{\gamma(T)}{\sqrt{Z(T)}} = \frac{\pi s}{2v_F}\frac{KT}{[1 - K\ln(\Delta_0/T)]^{5/2}}. \tag{79}$$

Using the parameters for BSCCO compounds [25,27–29], we estimate the ratio of the (isotropic) contribution of the energy diffusion channel [given by Eq. (77)] to the contribution of the local channel at its minimum:

$$\frac{\alpha_{d,d}}{(\alpha_{d,l})_{\min}} \approx 10, \quad f = 2\pi\omega \lesssim 1\ \mathrm{GHz}. \tag{80}$$

Here, we used the following values of relevant parameters: $n = 5\times10^{21}\ \mathrm{cm}^{-3}$, $v_F = 2.5\times10^7$ cm/s, $v_F/v_g = 20$, $T = 10$ K, impurity scattering rate $\gamma_0 = 1K$, and sound velocity $s = 4.6\times10^5$ cm/s.

VI. CONCLUSIONS

We have shown that low-frequency phonons in disordered conductors and superconductors experience additional damping due to the coupling between the lattice density modulations and a gas of thermally excited quasiparticles which is out of equilibrium with the lattice due to the finite frequency of the phonon-induced modulations. The nonequilibirum distribution of the quasiparticle energy then slowly decays leading to a phenomenon similar to the Mandelstam-Leontovich relaxation. The effect is especially strong in doped semiconductors at moderately low T/E_F and ultrasound frequencies $\omega \ll T/\hbar$. In particular, we have estimated the ultrasound attenuation in doped Si to be enhanced by a factor of about 100 due to this mechanism. The frequency dependence of the attenuation rate $\alpha(\omega)$ contains a typical crossover frequency ω_c, see Eq. (17), which depends explicitly on the electron diffusion coefficient D. Thus, measurements of $\alpha(\omega)$ may be used for the determination of D. A similar phenomenon exists in superconductors as well; for conventional s-wave superconductors, it is weak usually, but can be important for very low-density materials close to the BCS-BEC crossover, like the recently discovered YPtBi superconductor. For d-wave superconductors, we calculated both the conventional (local) and the diffusion-induced attenuation rate and showed that the latter may dominate in strongly anisotropic BSCCO materials at moderate temperatures. The possibility to extract electron parameters such as the diffusion coefficient D from measurements of $\alpha(\omega)$ in a d-wave case is especially interesting, since they posses nontrivial dependencies on temperature and disorder, due to the quantum criticality of a d-wave state.

ACKNOWLEDGMENTS

We are grateful to V. E. Kravtsov for useful discussions. This research was supported by the Russian Foundation for Basic Research grant 13-02-00963.

APPENDIX A: CANONICAL TRANSFORMATION

As Tsuneto had pointed out [4], in the linear approximation, the transition to a comoving frame of reference can be considered as a canonical transformation:

$$U = \exp\left(\frac{i}{2}\{\boldsymbol{u}_\alpha, \boldsymbol{p}_\alpha\}\right). \tag{A1}$$

This transformation is connected to the spatial translation $\boldsymbol{r} \to \boldsymbol{r} - \boldsymbol{u}$, with the exception that it conserves probability, $\psi(\boldsymbol{r}) \to (1 + (1/2)\mathrm{div}\,\boldsymbol{u})\psi(\boldsymbol{r} - \boldsymbol{u})$. The transition to CFR in normal conductors had already been considered in details, see Refs. [3–5,8,14,15]. It is a very general approach and here we

illustrate the way it works in an s-wave superconductor. It is convenient to introduce a particle-hole space that together with spin constitute the Nambu-Gorkov space. We introduce it in the exact same way as in the main text, so that the electron action is

$$S_{\mathrm{el},s} = \int dt(d\boldsymbol{r})\overline{\Psi}[\varepsilon\check{\tau}_3 - \xi(\boldsymbol{p})\check{\tau}_0 - \Delta(i\check{\tau}_2) - U(\boldsymbol{r})]\Psi, \tag{A2}$$

$$S_{\text{el-ph}} = \int dt(d\boldsymbol{r})\overline{\Psi}[-(p_F v_F/d)\,\mathrm{div}\,\mathbf{u} + \nabla_\alpha(u_\alpha U(\boldsymbol{r}))]\Psi. \tag{A3}$$

The first two terms of Eq. (A2) give a standard vertex,

$$\check{\Gamma}_0^{\alpha\beta} = [\varepsilon\check{\tau}_3 - \xi(\boldsymbol{p})\check{\tau}_0, \{u_\alpha, p_\alpha\}] \tag{A4}$$

$$= \dot{u}_\alpha p_\alpha \check{\tau}_3 - (i\nabla_\beta u_\alpha) p_\alpha v_\beta \check{\tau}_0, \tag{A5}$$

which after careful consideration of the screening together with the first term of Eq. (A3) becomes

$$\check{\Gamma}_n^{\alpha\beta} = \dot{u}_\alpha p_\alpha \check{\tau}_3 - (i\nabla_\beta u_\alpha)(p_\alpha v_\beta - (p_F v_F/d)\delta_{\alpha\beta}). \tag{A6}$$

The first term in the last equation is irrelevant in most of the cases due to the fact that $\omega \ll q v_F$.

The last terms of Eqs. (A2) and (A3) almost cancel out leaving

$$\check{\Gamma}_{\mathrm{imp}}^{\alpha\beta} = [U\check{\tau}_0, \{u_\alpha, p_\alpha\}] - \nabla_\alpha(u_\alpha U)\check{\tau}_0 = (U\,\mathrm{div}\,\mathbf{u})\check{\tau}_0. \tag{A7}$$

This term is inevitable in any reference frame since the scattering rate is the same in any reference frame and it depends on the concentration of impurities (provided we do not involve time transformations).

Last but not least, the second term of Eq. (A2) is

$$\check{\Gamma}_\Delta^{\alpha\beta} = [\check{\Delta}, \{u_\alpha, p_\alpha\}]. \tag{A8}$$

In the linear approximation, this gives

$$(i\check{\tau}_2)[\check{\Delta}, u_\alpha]p_\alpha + [\check{\Delta}, p_\alpha]u_\alpha \tag{A9}$$

$$= \partial_\beta u_\alpha(\partial\check{\Delta}/\partial p_\beta) + u_\alpha\nabla_\alpha\check{\Delta}. \tag{A10}$$

The first term is zero for the s-wave case but is essential for a d wave. The second term describes coupling to order parameter fluctuations and is not relevant for the problem considered in this paper.

Finally, as we have mentioned in the main text, an acoustic wave could change the effective BCS coupling constant. After screening by a SC propagator, we eventually get

$$\check{\Lambda} = \Delta(i\check{\tau}_2)\left(\frac{\partial\ln\Delta}{\partial\ln\rho}\right)_{\mathrm{el}}\mathrm{div}\,\mathbf{u}. \tag{A11}$$

This vertex represents changes in the order parameter as a result of the induced changes of the electronic DOS under strain. A similar contribution might arise from changes in the interaction constant itself so that

$$\frac{d\ln\Delta}{d\ln\rho} = \left(\frac{\partial\ln\Delta}{\partial\ln\rho}\right)_{\mathrm{el}} + \left(\frac{\partial\ln\Delta}{\partial\ln\rho}\right)_{\mathrm{lattice}}. \tag{A12}$$

APPENDIX B: EFFECTIVE ELECTRON-PHONON VERTEX IN A d-WAVE STATE

In the main text, we have used the tensorlike electron-phonon vertex,

$$(\check{S}_{\text{el-ph}})_1 = \int (d\boldsymbol{r})\overline{\psi}(p_\alpha\partial_\beta\check{H} - (p_F v_F/d)\delta_{\alpha\beta})\partial_\beta u_\alpha\psi. \tag{B1}$$

However, as we have just mentioned in Appendix A, careful calculation shows that the actual electron-phonon interaction in a comoving reference frame contains an additional contribution [8],

$$\check{S}_{\text{el-ph}} = (\check{S}_{\text{el-ph}})_1 + (\check{S}_{\text{el-ph}})_2, \tag{B2}$$

$$(\check{S}_{\text{el-ph}})_2 = \int (d\boldsymbol{r})\overline{\psi}[-U(\boldsymbol{r})(\partial_\alpha u_\alpha)]\psi. \tag{B3}$$

This contribution describes changes in the disorder potential *strength*, for example, changes in the local concentration of impurities. This term is usually negligible. However, this is not the case for a d-wave state, where it plays an important role.

1. Naive (incomplete) effective vertex

Let us first show what would be obtained for an effective phonon-diffuson vertex ignoring the disorder-related contribution. Taking into account only $(\check{H}_{\text{el-ph}}^{\mathrm{CFR}})_1$, we have

$$\langle\check{\Gamma}\rangle_{d1}^{\alpha\beta} = u\sum_{\text{nodes}}\int (dp)\check{G}_+^R(p_\alpha\partial_\beta\check{H} - (p_F v_F/d)\delta_{\alpha\beta})\check{G}_-^A. \tag{B4}$$

For longitudinal phonons, after the summation over the nodes is performed, the relevant terms arising from the vertex are

$$\sum_{\text{nodes}}(p_\alpha\partial_\beta\check{H} - (p_F v_F/d)\delta_{\alpha\beta}) = 2(\xi\check{\tau}_0 + \Delta(i\check{\tau}_2))\delta_{\alpha\beta}. \tag{B5}$$

We omit $\delta_{\alpha\beta}$ and α,β indices for brevity. The $\xi\check{\tau}_0$ term, for example, gives

$$\langle\check{\Gamma}\rangle_{d1a}(\varepsilon) = u\int (d\boldsymbol{p})\frac{2\xi^2\tilde{\varepsilon}\check{\tau}_3}{((\varepsilon_k - \tilde{\varepsilon})^2 + \gamma^2)^2} \tag{B6}$$

$$= \tilde{\varepsilon}(\varepsilon)\left(1 - \frac{1}{2}Z(\varepsilon)\right)\check{\tau}_3, \tag{B7}$$

where $\varepsilon_k = \sqrt{\xi^2 + \Delta^2}$. The same contribution arises from the $\Delta(i\check{\tau}_2)$ term thus resulting in

$$\langle\check{\Gamma}\rangle_{d1}(\varepsilon) = \tilde{\varepsilon}(\varepsilon)(2 - Z(\varepsilon))\check{\tau}_3. \tag{B8}$$

In the general case, the vertex (B8) depends on electron energy in a sophisticated way. Meanwhile, in the clean limit, when the impurities are negligible and $\tilde{\varepsilon}(\varepsilon) \to \varepsilon$, $Z(\varepsilon) \to 1$, we would have a very simple result: $\langle\check{\Gamma}\rangle_{d1} = \varepsilon\check{\tau}_3$. It turns out that this is in fact the correct answer once everything is taken into account.

2. Full effective vertex

What we have just left out is $(\check{S}_{\text{el-ph}})_2$, the disorder-induced contribution to the electron-phonon interaction:

$$\langle\check{\Gamma}\rangle_{d2}^{\alpha\beta} = u\sum_{\text{nodes}}\int (dp)\check{G}_+^R(U)\check{G}_-^A. \tag{B9}$$

After we average this vertex over the disorder we see that it gives

$$\begin{aligned}\langle\check{\Gamma}\rangle_{d2} &= u\sum_{\text{nodes}}\int (dp)\check{G}^R_+\big(\check{\Sigma}^R+\check{\Sigma}^A\big)\check{G}^A_- \\ &= \dots \\ &= 2\,\mathrm{Re}\,\check{\Sigma}^R = 2(\varepsilon-\tilde{\varepsilon}(\varepsilon))\check{\tau}_3. \end{aligned} \tag{B10}$$

In other words, this vertex is tightly connected to the renormalization of the electron energy. If the energy is not renormalized then this vertex is absent.

Recalling the relation $\varepsilon = Z(\varepsilon)\tilde{\varepsilon}(\varepsilon)$, we now see that the actual effective phonon-diffuson vertex is indeed connected only to the true electron energy variable ε:

$$\langle\check{\Gamma}\rangle_{d1} = (2\tilde{\varepsilon}-\varepsilon)\check{\tau}_3, \quad \langle\check{\Gamma}\rangle_{d2} = (2\varepsilon-2\tilde{\varepsilon})\check{\tau}_3, \tag{B11}$$

so that

$$\langle\check{\Gamma}\rangle_{d} = \langle\check{\Gamma}\rangle_{d1} + \langle\check{\Gamma}\rangle_{d2} = \varepsilon\check{\tau}_3, \tag{B12}$$

exactly the expression that was used in the main text.

APPENDIX C: KELDYSH TECHNIQUE

Despite the fact that Ref. [19] provides a pedagogical and detailed introduction into the Keldysh technique, we present here an example of calculations considering one of the diagrams from the main text, namely the energy diffusion contribution in the s-wave case.

We seek the imaginary part of the phonon self-energy, which is given by the expression

$$\Sigma^A = \mathrm{Tr}\,[\check{G}_-\check{\Gamma}^{(cl)}\check{G}_+,\check{\Gamma}^{(q)}], \tag{C1}$$

where the trace is taken over all spaces: Keldysh, spin, and particle-hole. $\pm$ indices stand for $(\varepsilon \pm \omega/2, \boldsymbol{p} \pm \boldsymbol{q}/2)$ arguments while (cl) and (q) stand for classical and quantum Keldysh vertices. Green function $\check{G}$ is a matrix in Keldysh space:

$$\check{G} = \begin{pmatrix} \check{G}^R & \check{G}^K \\ 0 & \check{G}^A \end{pmatrix}, \tag{C2}$$

with $\check{G}^R$, $\check{G}^A$, $\check{G}^K$ themselves being matrices in the Nambu-Gorkov space. After taking the trace over the Keldysh space, the expression for the phonon self-energy reduces to

$$\Sigma^A = \frac{q^2}{2}\mathrm{Tr}\,[\check{G}^R_-\check{\Gamma}\check{G}^K_+,\check{\Gamma} + \check{G}^K_-\check{\Gamma}\check{G}^A_+,\check{\Gamma}]. \tag{C3}$$

An extra q^2 factor appeared since in our definitions we actually exclude the phonon momentum from the definition of the vertex. Say, our vertex would be $p_\alpha v_\beta$, not $u_\alpha p_\alpha v_\beta q_\beta$. In equilibrium, $\check{G}^K = \check{G}^R\check{F} - \check{F}\check{G}^A = f(\varepsilon)(\check{G}^R - \check{G}^A)$ with $f(\varepsilon) = \tanh\varepsilon/2T$ and thus for the imaginary part of the self-energy, we obtain

$$\mathrm{Im}\,\Sigma^A = \frac{q^2}{4}\mathrm{Tr}\,[(f_+ - f_-)(\check{G}^R_- - \check{G}^A_-)\check{\Gamma}(\check{G}^R_+ - \check{G}^A_+)\check{\Gamma}], \tag{C4}$$

$$\mathrm{Im}\,\Sigma^A = \frac{q^2}{4}\,\mathrm{Re}\,(\mathrm{Tr}\,[\check{\Gamma}\check{G}^R_-\check{\Gamma}\check{G}^R_+ - \check{\Gamma}\check{G}^A_-\check{\Gamma}\check{G}^R_+]). \tag{C5}$$

Dealing with ultrasound we assume that the frequency is low, $\hbar\omega \ll T$, so expanding the expression above to linear order in ω and using the relation (6) between α and $\mathrm{Im}\,\Sigma^A$, we get $f(\varepsilon) = \tanh\varepsilon/2T$ and thus for the imaginary part of the self-energy, we obtain

$$\alpha_s(\omega) = \int_0^\infty \left(d\varepsilon\frac{\partial f(\varepsilon,T)}{\partial\varepsilon}\right)\alpha_s^{(\varepsilon)}(\omega), \tag{C6}$$

where $\alpha_s^{(\varepsilon)}(\omega)$ is the contribution to the attenuation from electrons with energies in an interval $(\varepsilon,\varepsilon+d\varepsilon)$,

$$\alpha_s^{(\varepsilon)}(\omega) = \frac{q^2}{4\rho_m}\mathrm{Tr}^{(\varepsilon)}[(\check{G}^R_- - \check{G}^A_-)\check{\Gamma}(\check{G}^R_+ - \check{G}^A_+)\check{\Gamma}], \tag{C7}$$

where the trace is now taken over momenta and the Nambu-Gorkov space (at a chosen electron energy ε). Dealing with a disordered system we have yet to take an average over the disorder. We skip the arising local part, focusing on the diffusive part that corresponds to the diagrams with noncrossing impurity lines connecting two Greens functions. If we sum all such diagrams, we obtain a whole impurity ladder that is connected to a diffusion mode.

It is evident from Eq. (C7) that two kinds of terms exist: AR and RR types. The first gives the diffuson's contribution, while the second describes the Cooperon modes. The presence of a diffusive dynamic contribution from the R-R combination might be confusing; it is due to the fact that the retarded matrix Green function is a combination of a retarded particle propagator at energy ε and an advanced hole propagator taken at energy $-\varepsilon$,

$$\check{G}^R(\varepsilon,\boldsymbol{p})|_{\Delta=0} = \begin{pmatrix} G_0^R(\varepsilon,\boldsymbol{p}) & 0 \\ 0 & -G_0^A(-\varepsilon,-\boldsymbol{p}) \end{pmatrix}, \tag{C8}$$

where for clarity, we had ignored the anomalous part of the propagator. The combination $G^R(\varepsilon,\boldsymbol{p})G^A(-\varepsilon,-\boldsymbol{p})$ corresponds to the Cooperon mode. Below, we show that the R-R part is indeed irrelevant, as we have stated in the main text. Since only the $\check{\Gamma}^{AR}$ vertex is relevant for the problem, we did not keep the superscript AR in the main text, but below we keep it to avoid possible confusion.

As we have stated in the main text, it is very convenient to introduce an effective phonon-diffuson vertex that describes the coupling between an acoustic wave and diffusion modes. We see from the diagram that we have two blocks of two Green functions near each phonon vertex. For A-R, the diagram gives

$$\alpha^{(\varepsilon)}_{s,d,AR}(\omega) = \frac{1}{4\rho_m u}\,\mathrm{Re}\,(\mathrm{tr}\,[\langle\check{\Gamma}\rangle^\dagger_{s,AR}\underline{\widehat{\mathcal{D}}}\langle\check{\Gamma}\rangle_{s,AR}]), \tag{C9}$$

where the trace is now taken only over the Nambu-Gorkov space, the effective vertex is defined in exactly the same way as in the main text:

$$\langle\check{\Gamma}\rangle_{s,AR}(\varepsilon) = u\int (d\,\boldsymbol{p})\check{G}^R_-\Gamma_n(\boldsymbol{p}_-,\boldsymbol{p}_+)\check{G}^A_+, \tag{C10}$$

and $\underline{\widehat{\mathcal{D}}}$ is a superoperator corresponding to the diffuson, the sum of the impurity ladder

$$\underline{\widehat{\mathcal{D}}}(\varepsilon,\omega,\boldsymbol{q}) = \left[1 - u\int (d\,\boldsymbol{p})\check{G}^A(\varepsilon_+,\boldsymbol{p}_+)\otimes\check{G}^R(\varepsilon_-,\boldsymbol{p}_-)\right]^{-1}. \tag{C11}$$

The action of a superoperator $\check{G}^A \otimes \check{G}^R$ is defined as

$$(\check{G}^A \otimes \check{G}^R)\langle\check{\Gamma}\rangle = \check{G}^A\langle\check{\Gamma}\rangle\check{G}^R. \tag{C12}$$

In Eq. (C9), we have an extra factor u^{-1} in front of the trace since we exclude one impurity line from the definition of the diffuson (C11) (the impurity ladder series starts from 1, not u) yet include one into each effective vertex (C10). Hence $u(u)^{-2} = u^{-1}$. Since the structure of the vertex in an acoustic wave polarization space is trivial $\sim \delta_{\alpha\beta}$, we omit here all these extra indices. The effective vertex introduced in this way is tightly connected to the vertex of the type $\mathrm{Tr}\,[\widehat{Q}\,\mathrm{div}\,\mathbf{u}]$ in the nonlinear sigma-model approach to disordered conductors [19].

Before moving forward, we remind that the retarded Green function in the s-wave state as follows from Eq. (20) is

$$\check{G}^R(\varepsilon,\boldsymbol{p}) = \frac{\eta_\varepsilon(\varepsilon\check{\tau}_3 - \Delta(i\check{\tau}_2)) + \xi\check{\tau}_0}{\eta^2E^2 - \xi^2} \tag{C13}$$

with $\eta_\varepsilon = 1 + i/2\tau E, E = \sqrt{\varepsilon^2 - \Delta^2}$.

1. $A-R$ diffuson and effective vertex

a. Diffuson

To evaluate the diffusion propagator, we have to calculate the diffuson self-energy

$$\underline{\check{\Xi}}(\varepsilon,\omega,\boldsymbol{q}) = \int (d\,\boldsymbol{p})\check{G}^A(\varepsilon_+,\boldsymbol{p}_+) \otimes \check{G}^R(\varepsilon_-,\boldsymbol{p}_-). \tag{C14}$$

We first seek the eigenmodes of the diffuson. Since we interpret $\widehat{\underline{\Xi}}$ as a superoperator, appropriate eigenmodes correspond to eigenoperators of a superoperator. The Pauli matrices $\check{\tau}_i$, $i = 0,\ldots,3$ provide a basis in the operator space and any eigenopertor will be some combination of Pauli matrices. For zero external $\omega, v_Fq = 0$, we thus have

$$\underline{\check{\Xi}} = u\int \nu d\xi \frac{\eta^*_\varepsilon(\varepsilon\check{\tau}_3 - \Delta(i\check{\tau}_2)) + \xi\check{\tau}_0}{((\eta^*_\varepsilon)^2E^2 - \xi^2)} \otimes \ldots \tag{C15}$$

$$\ldots \otimes \frac{\eta_\varepsilon(\varepsilon\check{\tau}_3 - \Delta(i\check{\tau}_2)) + \xi\check{\tau}_0}{(\eta^2_\varepsilon E^2 - \xi^2)} \tag{C16}$$

that reduces to

$$\underline{\check{\Xi}} = \frac{(\varepsilon\check{\tau}_3 - \Delta(i\check{\tau}_2)) \otimes (\varepsilon\check{\tau}_3 - \Delta(i\check{\tau}_2))}{E^2} I_{\mathcal{D}1} + \check{\tau}_0 \otimes \check{\tau}_0 I_{\mathcal{D}2} \tag{C17}$$

with integrals $I_{\mathcal{D}1}$ and $I_{\mathcal{D}2}$,

$$I_{\mathcal{D}1} = u\int \nu d\xi \frac{|\eta|^2E^2}{\left|\eta^2_\varepsilon E^2 - \xi^2\right|^2} = \frac{1}{2}, \tag{C18}$$

$$I_{\mathcal{D}2} = u\int \nu d\xi \frac{\xi^2}{\left|\eta^2_\varepsilon E^2 - \xi^2\right|^2} = \frac{1}{2}, \tag{C19}$$

where we had used the fact that $u = (2\pi\nu\tau)^{-1}$. We have thus

$$\underline{\check{\Xi}} = \frac{1}{2}\check{\tau}_0 \otimes \check{\tau}_0 + \frac{(\varepsilon\check{\tau}_3 - \Delta(i\check{\tau}_2)) \otimes (\varepsilon\check{\tau}_3 - \Delta(i\check{\tau}_2))}{2E^2} \tag{C20}$$

and the eigenoperators corresponding to massless modes (with eigenvalues $\Xi = 1$ and thus $\mathcal{D}^{-1} = 0$) are

$$\text{massless:}\quad \check{\tau}_0 \quad\text{and}\quad \frac{1}{E}(\varepsilon\check{\tau}_3 - \Delta(i\check{\tau}_2)) \tag{C21}$$

charge and energy. The remaining massive eigenoperators are

$$\text{massive:}\quad \check{\tau}_1 \quad\text{and}\quad \frac{1}{E}(\varepsilon\check{\tau}_3 + \Delta(i\check{\tau}_2)) \tag{C22}$$

with eigenvalues $\Xi = 0$. These do not describe any diffusion modes, they are akin to a G^RG^R combination in the normal metal where the impurity ladder cannot be inserted.

We consider a finite ω, v_Fq in the spirit of perturbation theory, when an eigenvalue can be obtained by an average over the eigenstate in the zero-order approximation,

$$\Xi^{(\varepsilon)}_i(\omega,\boldsymbol{q}) = \frac{1}{2}\mathrm{tr}\,[\check{\tau}_i\underline{\check{\Xi}}\check{\tau}_i] = u\int (d\,\boldsymbol{p})\frac{1}{2}\mathrm{tr}\,[\check{\tau}_i\check{G}^A_+\check{\tau}_i\check{G}^R_-]. \tag{C23}$$

It is easy to see that the eigenvalue for $\check{\tau}_0$ and $\varepsilon\check{\tau}_3 + \Delta(i\check{\tau}_2)$ is the same, since they both commute with self-energy $\underline{\check{\Xi}}$ at $\omega = 0$. Say for charge we have

$$\Xi^{(\varepsilon)}_0(\omega,\boldsymbol{q}) = u\int (d\,\boldsymbol{p})\frac{1}{2}\mathrm{tr}\left[\frac{(\eta_+\varepsilon_+)(\eta^*_-\varepsilon_-) - \Delta^2) - \xi_+\xi_-}{(\eta^*_+)^2E^2_+ - \xi^2_+)(\eta^2_-E^2_- - \xi^2_-)}\right] \tag{C24}$$

$$= 1 - [-i(E_+ - E_-) + Dq^2], \tag{C25}$$

where we had expanded in ω,q and $D = (1/d)\tau v_F^2$ is a diffusion coefficient in a *normal* state. The diffuson is thus

$$\mathcal{D}^{(\varepsilon)}(\omega,\boldsymbol{q}) = \frac{1}{-i(E_+ - E_-) + Dq^2}. \tag{C26}$$

Note that in order to obtain the true diffusion coefficient in the *s-wave* state, we have to expand $E_+ - E_-$ in ω,

$$\frac{1}{-i(E_+ - E_-) + Dq^2} = \frac{\sqrt{\varepsilon^2 - \Delta^2}}{\varepsilon}\frac{1}{-i\omega + D^{(\varepsilon)}_s q^2} \tag{C27}$$

with a diffusion coefficient in the s-wave state

$$D^{(\varepsilon)}_s = \frac{\sqrt{\varepsilon^2 - \Delta^2}}{\varepsilon}D \equiv \frac{\nu_n}{\nu_s(\varepsilon)}D. \tag{C28}$$

b. Effective vertex

For the effective vertex, we have

$$\langle\check{\Gamma}\rangle_{s,AR}(\varepsilon) = u\int (d\,\boldsymbol{p})\frac{[\eta_\varepsilon(\varepsilon\check{\tau}_3 - \Delta(i\check{\tau}_2)) + \xi\check{\tau}_0]}{\left(\eta^2_\varepsilon E^2 - \xi^2\right)} \times [\varkappa\xi\check{\tau}_0] \times \frac{[\eta^*_\varepsilon(\varepsilon\check{\tau}_3 - \Delta(i\check{\tau}_2)) + \xi\check{\tau}_0]}{\left(\eta^2_\varepsilon E^2 - \xi^2\right)^*}, \tag{C29}$$

giving

$$\langle\check{\Gamma}\rangle_{s,AR}(\varepsilon) = 2\varkappa I_{\mathcal{D}2}(\varepsilon\check{\tau}_3 - \Delta(i\check{\tau}_2)), \tag{C30}$$

where $I_{\mathcal{D}2}$ is exactly the same as given by Eq. (C38), leading to

$$\langle\check{\Gamma}\rangle_{s,AR}(\varepsilon) = \varkappa(\varepsilon\check{\tau}_3 - \Delta(i\check{\tau}_2). \tag{C31}$$

Similarly, $\check{\Lambda} = \varkappa_\Delta \Delta(i\check{\tau}_2)$ gives

$$\langle\check{\Lambda}\rangle_{s,AR}(\varepsilon) = (\varkappa_\Delta\Delta)\left(I_{\mathcal{D}1} - \frac{\varepsilon^2+\Delta^2}{E^2} I_{\mathcal{D}2}\right)(i\check{\tau}_2) \quad \text{(C32)}$$

$$= \varkappa_\Delta\left(-\frac{\Delta^2}{E^2}\right)\Delta(i\check{\tau}_2), \quad \text{(C33)}$$

where $I_{\mathcal{D}1}, I_{D2}$ are given by Eqs. (C37) and (C38). Finally, $(i\check{\tau}_2)$ gives a superposition of massless (C20) and massive (C39) modes,

$$\Delta(i\check{\tau}_2) = \frac{\varepsilon\check{\tau}_3 + \Delta(i\check{\tau}_2)}{2} - \frac{\varepsilon\check{\tau}_3 - \Delta(i\check{\tau}_2)}{2}. \quad \text{(C34)}$$

Only the massless mode is of interest for us. Projecting onto the massless subspace, we obtain

$$\langle\check{\Lambda}\rangle_{s,AR}(\varepsilon) = \varkappa_\Delta \frac{\Delta^2}{2(\varepsilon^2-\Delta^2)}(\varepsilon\check{\tau}_3 - \Delta(i\check{\tau}_2)), \quad \text{(C35)}$$

Eventually, we have to use our effective vertices and diffuson in Eq. (C9), exactly what was done in the main text.

2. *R-R* diffuson (Cooperon) and effective vertex

In the case of a Cooper mode, the calculations are absolutely similar to the diffuson case up to the use of RR combinations instead of RA. For the self-energy we have

$$\underline{\check{\Xi}}_{\mathcal{C}} = \frac{(\varepsilon\check{\tau}_3 - \Delta(i\check{\tau}_2)) \otimes (\varepsilon\check{\tau}_3 - \Delta(i\check{\tau}_2))}{E^2} I_{\mathcal{C}1} + \check{\tau}_0 \otimes \check{\tau}_0 I_{\mathcal{C}2} \quad \text{(C36)}$$

with integrals

$$I_{\mathcal{C}1} = u\int \nu d\xi \frac{\eta^2 E^2}{\left(\eta_\varepsilon^2 E^2 - \xi^2\right)^2} = \frac{1}{2(1-2i\tau E)}, \quad \text{(C37)}$$

$$I_{\mathcal{C}2} = u\int \nu d\xi \frac{\xi^2}{\left(\eta_\varepsilon^2 E^2 - \xi^2\right)^2} = \frac{1}{2(1-2i\tau E)}. \quad \text{(C38)}$$

This results in the same set of eigenoperators:

$$\text{massless:} \quad \check{\tau}_0 \quad \text{and} \quad \frac{1}{E}(\varepsilon\check{\tau}_3 - \Delta(i\check{\tau}_2)), \quad \text{(C39)}$$

$$\text{massive:} \quad \check{\tau}_1 \quad \text{and} \quad \frac{1}{E}(\varepsilon\check{\tau}_3 + \Delta(i\check{\tau}_2)), \quad \text{(C40)}$$

and a Cooperon eigenvalue similar to a diffuson,

$$\mathcal{C}^{(\varepsilon)}(\omega,\boldsymbol{q}) = \frac{1}{i(E_+ + E_-) + Dq^2}. \quad \text{(C41)}$$

Unsurprisingly, the expressions for the effective vertices are obtained as well by a modification of the integrals $I_{\mathcal{D}i} \to I_{\mathcal{C}i}$. Given that we always have $\tau E \ll 1$, the modification of the effective vertex as compared to the AR case is negligible, and RR vertex turns out to be the same as AR,

$$\langle\check{\Gamma}\rangle_{s,RR}(\varepsilon) \simeq \langle\check{\Gamma}\rangle_{s,AR}(\varepsilon), \quad \text{(C42)}$$

and same for the $\check{\Lambda}$ vertex.

The gap in a Cooperon propagator (C41) suppresses the contribution from this mode in the limit $Dq^2 \ll \sqrt{T\Delta}$. On the other hand, in the opposite limit, $Dq^2 \gtrsim \sqrt{T\Delta}$, the contribution from a Cooper mode is the same as that of the diffuson resulting in an additional overall factor of 2.

[1] A. B. Pippard, CXXII. Ultrasonic attenuation in metals, Philos. Mag. **46**, 1104 (1955).

[2] A. I. Akhiezer, M. I. Kaganov, and G. Ya. Lyubarskyi, Ultrasound absorption in metals, Zh. Eksp. Teor. Fiz. **32**, 837 (1957) [Sov. Phys. JETP **5**, 685 (1957)].

[3] E. I. Blount, Ultrasonic attenuation by electrons in metals, Phys. Rev. **114**, 418 (1959).

[4] T. Tsuneto, Ultrasonic attenuation in superconductors, Phys. Rev. **121**, 402 (1960).

[5] A. Schmid, Electron-phonon interaction in an impure metal, Z. Phys. **259**, 421 (1973).

[6] H. Frohlich, Theory of the superconducting state. I. The ground state at the absolute zero of temperature, Phys. Rev. **79**, 845 (1950).

[7] A. B. Migdal, Interaction between electrons and lattice vibrations in a normal metal, Zh. Eksp. Teor. Fiz. **34**, 1438 (1958) [Sov. Phys. JETP **7**, 996 (1958)].

[8] A. V. Shtyk, M. V. Feigel'man, and V. E. Kravtsov, Magnetic Field-Induced Giant Enhancement of Electron-Phonon Energy Transfer in Strongly Disordered Conductors, Phys. Rev. Lett. **111**, 166603 (2013).

[9] B. L. Altshuler, V. E. Kravtsov, I. V. Lerner, and I. L. Aleiner, Jumps in Current-Voltage Characteristics in Disordered Films, Phys. Rev. Lett. **102**, 176803 (2009).

[10] M. Ovadia, B. Sacépé, and D. Shahar, Electron-Phonon Decoupling in Disordered Insulators, Phys. Rev. Lett. **102**, 176802 (2009).

[11] M. E. Gershenson, Yu. B. Khavin, D. Reuter, P. Schafmeister, and A. D. Wieck, Hot-Electron Effects in Two-Dimensional Hopping with a Large Localization Length, Phys. Rev. Lett. **85**, 1718 (2000).

[12] A. Savin, J. Pekola, M. Prunnila, J. Ahopelto, and P. Kivinen, Electronic cooling and hot electron effects in heavily doped silicononinsulator film, Phys. Scr. **T114**, 57 (2004).

[13] M. Prunnila, Electron–acoustic-phonon energy-loss rate in multicomponent electron systems with symmetric and asymmetric coupling constants, Phys. Rev. B **75**, 165322 (2007).

[14] A. Sergeev and V. Mitin, Electron-phonon interaction in disordered conductors: Static and vibrating scattering potentials, Phys. Rev. B **61**, 6041 (2000).

[15] A. Sergeev, M. Y. Reizer, and V. Mitin, Deformation Electron-Phonon Coupling in Disordered Semiconductors and Nanostructures, Phys. Rev. Lett. **94**, 136602 (2005).

[16] O. Vafek and Z. Tešanović, Quantum criticality of d-wave quasiparticles and superconducting phase fluctuations, Phys. Rev. Lett. **91**, 237001 (2003).

[17] L. V. Keldysh, Diagram technique for nonequilibrium processes, Zh. Eksp. Teor. Fiz. **47**, 1515 (1964) [Sov. Phys. JETP **20**, 1018 (1965)].

[18] J. Rammer and H. Smith, Quantum field-theoretical methods in transport theory of metals, Rev. Mod. Phys. **58**, 323 (1986).

[19] A. Kamenev and A. Levchenko, Keldysh technique and nonlinear ϕ-model: basic principles and applications, Adv. Phys. **58**, 197 (2009).

[20] A. A. Abrikosov, L. P. Gorâkov, and I. E. Dzyaloshinskii, Quantum Field Theoretical Methods in Statistical Physics, *Quantum Field TheoreticalMethods in Statistical Physics* (Oxford, 1965).

[21] M. Tinkham, Introduction to Superconductivity, *Introduction to Superconductivity* (Dover, 2004).

[22] N. P. Butch, P. Syers, K. Kirshenbaum, A. P. Hope, and J. Paglione, Superconductivity in the topological semimetal YPtBi, Phys. Rev. B **84**, 220504 (2011).

[23] We estimate sound velocity of YPtBi with that of a bismuth.

[24] A. E. Koshelev and A. A. Varlamov, Mesoscopic variations of local density of states in disordered superconductors, Phys. Rev. B **85**, 214507 (2012).

[25] J. Mesot *et al.*, Superconducting Gap Anisotropy and Quasiparticle Interactions: A Doping Dependent Photoemission Study, Phys. Rev. Lett. **83**, 840 (1999).

[26] P. M. Ostrovsky, I. V. Gornyi, and A. D. Mirlin, Electron transport in disordered graphene, Phys. Rev. B **74**, 235443 (2006).

[27] G. Heine, W. Lang, X. L. Wang, and S. X. Dou, Positive in-plane and negative out-of-plane magnetoresistance in the overdoped high-temperature superconductor $Bi_2Sr_2CaCu_2O_{8+x}$, Phys. Rev. B **59**, 11179 (1999).

[28] L. Forro, D. Mandrus, C. Kendziora, L. Mihaly, and R. Reeder, Hall-effect measurements on superconducting and nonsuperconducting copper-oxide-based metals, Phys. Rev. B **42**, 8704 (1990).

[29] J. Dominec, Ultrasonic and related experiments in high-Tc superconductors, Supercond. Sci. Technol. **6**, 153 (1993).